AN ANALYSIS OF TROPOSPHERIC AEROSOL CONCENTRATION AND DISTRIBUTION USING NOAA AVHRR
(ANALISIS KEPEKATAN DAN TABURAN AEROSOL MENGGUNAKAN NOAA AVHRR)

WAN HAZLI WAN KADIR
AB LATIF BIN IBRAHIM
ABD WAHID BIN RASIB
MAZLAN HASHIM

RESEARCH VOT NO:
75102

Jabatan Remote Sensing
Fakulti Kejuruteraan dan Sains Geoinformasi
Universiti Teknologi Malaysia

2007

UNIVERSITI TEKNOLOGI MALAYSIA

BORANG PENGESAHAN
LAPORAN AKHIR PENYELIDIKAN

TAJUK PROJEK : AN ANALYSIS OF TROPOSPHERIC AEROSOL CONCENTRATION AND DISTRIBUTION USING NOAA AVHRR

Saya WAN HAZLI BIN WAN KADIR
(HURUF BESAR)

Mengaku membenarkan **Laporan Akhir Penyelidikan** ini disimpan di Perpustakaan Universiti Teknologi Malaysia dengan syarat-syarat kegunaan seperti berikut :

1. Laporan Akhir Penyelidikan ini adalah hakmilik Universiti Teknologi Malaysia.
2. Perpustakaan Universiti Teknologi Malaysia dibenarkan membuat salinan untuk tujuan rujukan sahaja.
3. Perpustakaan dibenarkan membuat penjualan salinan Laporan Akhir Penyelidikan ini bagi kategori TIDAK TERHAD.
4. * Sila tandakan (/)

☐	SULIT	(Mengandungi maklumat yang berdarjah keselamatan atau Kepentingan Malaysia seperti yang termaktub di dalam AKTA RAHSIA RASMI 1972).
☐	TERHAD	(Mengandungi maklumat TERHAD yang telah ditentukan oleh Organisasi/badan di mana penyelidikan dijalankan).
☑	TIDAK TERHAD	

TANDATANGAN KETUA PENYELIDIK

Nama & Cop Ketua Penyelidik

Tarikh : _____

CATATAN : ***** *Jika Laporan Akhir Penyelidikan ini SULIT atau TERHAD, sila lampirkan surat daripada pihak berkuasa/organisasi berkenaan dengan menyatakan sekali sebab dan tempoh laporan ini perlu dikelaskan sebagai SULIT dan TERHAD.*

UNIVERSITI TEKNOLOGI MALAYSIA
Research Management Centre

PRELIMINARY IP SCREENING & TECHNOLOGY ASSESSMENT FORM

(To be completed by Project Leader submission of Final Report to RMC or whenever IP protection arrangement is required)

1. **PROJECT TITLE IDENTIFICATION** :

AN ANALYSIS OF TROPOSPHERIC AEROSOL CONCENTRATION AND DISTRIBUTION USING NOAA AVHRR

Vote No: **75102**

2. **PROJECT LEADER** :

Name: WAN HAZLI BIN WAN KADIR

Address: DEPARTMENT OF REMOTE SENSING, FACULTY OF GEOINFORMATION SCIENCE AND ENGINEERING ,UNIVERSITI TEKNOLOGI MALAYSIA SKUDAI, JOHOR

Tel : 5530668 Fax : 5566163 e-mail : wanhazli@fksg.utm.my

3. **DIRECT OUTPUT OF PROJECT** *(Please tick where applicable)*

Scientific Research	Applied Research	Product/Process Development
☐ Algorithm	☑ Method/Technique	☐ Product / Component
☐ Structure	☐ Demonstration / Prototype	☐ Process
☐ Data		☐ Software
☐ Other, please specify	☐ Other, please specify	☐ Other, please specify
_____	_____	_____
_____	_____	_____

4. INTELLECTUAL PROPERTY *(Please tick where applicable)*

☐ Not patentable
☐ Patent search required
☐ Patent search completed and clean
☐ Invention remains confidential
☐ No publications pending
☐ No prior claims to the technology
☐ Technology protected by patents
☐ Patent pending
☐ Monograph available
☐ Inventor technology champion
☐ Inventor team player
☐ Industrial partner identified

5. LIST OF EQUIPMENT BOUGHT USING THIS VOT

a. HP notebook

b. NOAA satellite data

6. STATEMENT OF ACCOUNT

a)	APPROVED FUNDING	RM : 18 000
b)	TOTAL SPENDING	RM : 18000
c)	BALANCE	RM : 0

7. TECHNICAL DESCRIPTION AND PERSPECTIVE

Please tick an executive summary of the new technology product, process, etc., describing how it works. Include brief analysis that compares it with competitive technology and signals the one that it may replace. Identify potential technology user group and the strategic means for exploitation.

a) Technology Description

This research presented the potential of extracting AOT map from low resolution data, NOAA-16 over Malaysia region. The high correlation is found between AOT values and PM_{10} measurement, which suggest that the application of DTA algorithm is best used on available and cloud free AVHRR imagery. In fact, the daily AOT maps indicate air quality information which are somehow minimizing the cost and time compared to the conservative observation.

b) Market Potential

The findings are extremely usèful to all Government agencies, particulary those in charge of environment monitoring such as Malaysian Departmrnt of Meteorlogy Malaysian Centre of Remote Sensing (MACRES) and Department of Fisheries.

c) Commercialisation Strategies

This work needs no commercialisation. Nevertheless, a monograph if published may be the only way to gain from this work.

Signature of Projet Leader :- Date :-

_____ _____

8. RESEARCH PERFORMANCE EVALUATION

a) FACULTY RESEARCH COORDINATOR

Research Status	( )	( )	( )	( )	( )	( )
Spending	( )	( )	( )	( )	( )	( )
Overall Status	( )	( )	( )	( )	( )	( )
	Excellent	Very Good	Good	Satisfactory	Fair	Weak

Comment/Recommendations :

_____

_____

_____

_____

_____

_____

…… Name : ……

Signature and stamp of JKPP Chairman

Date : ……

b) RMC EVALUATION

Research Status	( )	( )	( )	( )	( )	( )
Spending	( )	( )	( )	( )	( )	( )
Overall Status	( )	( )	( )	( )	( )	( )
	Excellent	Very Good	Good	Satisfactory	Fair	Weak

Comments :-

_____

_____

_____

_____

_____

_____

Recommendations :

☐ Needs further research

☐ Patent application recommended

☐ Market without patent

☐ No tangible product. Report to be filed as reference

…….. Name : …….

Signature and Stamp of Dean / Deputy Dean
Research Management Centre

Date : …….

AN ANALYSIS OF TROPOSPHERIC AEROSOL CONCENTRATION AND DISTRIBUTION USING NOAA AVHRR

WAN HAZLI WAN KADIR
AB LATIF BIN IBRAHIM
ABD WAHID BIN RASIB
MAZLAN HASHIM,

Report submitted to Research Management Centre as Fulfilment of
Research Funding Vot no. 75102

UNIVERSITI TEKNOLOGI MALAYSIA
FACULTY OF GEOINFORMATION SCIENCE & ENGINEERING

Nov 2007

ACKNOWLEDGEMENT

We would like to thank Ministry of Science Technology and Innovation (MOSTI) for the funding that have make this study possible. This fund would be a huge opportunity given by MOSTI for new technology such as Remote Sensing in Malaysia. Assistance rendered by Research Management Centre (RMC), of Universiti Teknologi Malaysia (UTM) is also highly acknowledged. We also like to thank Alam Sekitar Malaysia Berhad (ASMA) for their kindness in contributing *in situ* data in this research work.

In preparing this research, we made a contact and approach with many people, researchers, academicians and practitioners. They have contributed towards our understanding and thoughts.

ABSTRACT

The air quality indicator approximated by satellite measurements is known as atmospheric particulate loading, which is evaluated in terms of columnar optical thickness of aerosol scattering. The effect brought by particulate pollution has gained interest after recent evidence on health effects of small particles. This study presents the potentiality of using NOAA AVHRR data to obtain tropospheric aerosol distribution over Malaysian land area. Contrast reduction technique is used in order to extract the aerosol optical thickness (AOT). Differential textural analysis (DTA) algorithm is applied on the geometrically corrected images of NOAA AVHRR. The algorithm is applied onto three sequence years of NOAA AVHRR data. Correlation as high as 0.9567, 0.8633 and 0.8361 for respectively three sequence years, 2002, 2003 and 2004 are found between the retrieved AOT values and PM_{10} data. The results suggests that the application of DTA algorithm on NOAA AVHRR imagery whenever available and cloud free could be used as an indicator to air quality assessment for this region.

ABSTRAK

Aktiviti penganggaran kualiti udara yang diukur dari satelit atau dalam terma saintifiknya pengukuran muatan zarah di atmosfera, ditaksir daripada ketebalan optikal secara vertical oleh serakan aerosol. Beberpakajian di dalam bidang perubatan telah menunjukkan bukti kukuh tentang kesan negatif partikal ini kepada kesihatan manusia, seterusnya telah menarik minat ramai penyelidik untuk melakukan kajian tentang aerosol dengan lebih mendalam. Kajian ini telah dijalankan untuk mengetahui potensi data NOAA untuk mengukur jumlah taburan aerosol troposfera bagi kawasan darat di Malaysia. Teknik *contrast reduction* digunakan untuk mengekstrak nilai ketebalan optikal aerosol (AOT). *Differential Textural Analysis* (DTA) telah dijalankan ke atas imej *National Oceanic and Atmospheric Administration* (NOAA) *A Very High Resolution Radiometer* (AVHRR) yang telah dibetulkan geometrinya. Algoritma ini telah diaplikasikan ke atas 3 siri data NOAA AVHRR. Nilai korelasi yang tinggi iaitu 0.9567, 0.8633 dan 0.8361 telah diperolehi merujuk kepada 3 siri data yang berturutan iaitu 2002, 2003 dan 2004. analisis regressi ini telah dijalankan ke atas nilai AOT yang diekstrak dari imej satelit NOAA AVHRR dan data sokongan dari kerja lapangan, PM_{10}. Hasil kajian ini secara optimis telah membuktikan bahawa algoritma DTA amat praktikal untuk digunakan ke atas data NOAA AVHRR yang bebas dari pengaruh awan dan seterusnya boleh digunakan sebagai kayu ukur kualiti udara bagi kawasan kajian ini.

CONTENTS

LIST OF FIGURES

LIST OF TABLES

CHAPTER I

INTRODUCTION

1.1 Background

Aerosols are solid particles and remain suspended in the atmosphere at various sizes from 10^{-3}mm to 10^{3}mm (Ortiz *et al.*, 2003). All liquid or solid particles in the air that are not consisting of water are called aerosol. They were originated from natural and man-made sources. Natural aerosol contains coarse dust particles, widespread fine aerosol from volcano as in Figure 1.1(a), oceanic and continental sources. While man-made aerosol particles are produced from industrial activities and in urban areas by automobiles, cooking and vegetation fires as shown in Figure 1.1 (b).

The impact of aerosol in global climate system through the direct and indirect forces is one of the major uncertainties in presenting climate model (Hansen and Lacis, 1990; Charlson et al, 1992; Lacis and Mishchenko, 1995). Furthermore, aerosol plays an important role in atmospheric chemistry and hence effects the concentration of other key-role atmospheric constituents, such as ozone. Therefore knowledge of aerosol in physical and chemical properties is critically important for climate change and environmental studies.

(a) (b)

Figure 1.1: Sources of aerosols (a) Volcano; (b) Fossil burning from vehicle.

Aerosol particles scatter and absorb sun radiation. Absorption properties result in heating of the atmospheric layer that contains the aerosol, while scattering properties cause a redistribution of radiation including losses back to space. The direct radiative effect of aerosol depends on the single scattering albedo defined as the ratio of scattering to extinction coefficient of these particles. Haze and smog over megacities are caused by radiative effect of aerosol. The most commonly observed consequences of atmospheric aerosols are the blueness of the sky and the redness of sunset or sunrise. These phenomena result from the more highly efficient scattering of blue light than red light by small particles, as formulated by Rayleigh in 1871. In a sunset or sunrise, the red at end of the visible spectrum of the sun remains unscattered as it approaches an observer, while the blue at end of the spectrum is scattered and not observed.

Aerosols are categorized by their mode of size. There are three size modes, which is the nuclei mode for particles less than 0.04μm in diameter, the accumulation mode for particles between 0.04μm and 0.5μm in diameter, and the coarse mode for particles larger than 1.0μm in diameter. In determining the impact of aerosol particles on human health, the size of these particles is considered to be the primary

determining factor. Ultra fine particles, which are less than 1.0µm in diameter have a high potential to penetrate deeply into the respiratory tract causing inflammation and irritation (Reid and Sayer, 2002). While particulate matter that less than 10.0µm in diameter acts to increase the number of respiratory diseases, pulmonary diseases and cardio vascular diseases.

Acid rain was recognized as early as in the middle of 1950, which caused by combustion of fossil fuels. Usually, the pH of cloud droplets in clean unpolluted air could be as low as 5. However, atmospheric water in polluted air has pH of 5.6 due to dissolved carbon dioxide and the formation of weak acid, carbonic acid (Cofala et al., 2004).

Daily satellite observation and continuous *in situ* measurement are needed to observe the emission and transportion of dense aerosol plumes downwind in populated and polluted region. Satellite sensors quantify atmospheric and surface properties by measuring the wavelength, angular and polarization properties of radiant energy that reflected from the earth. Aerosol can be seen clearly in high resolution satellite as shown in Figure 1.2.

Figure 1.2: Cloud and aerosol in satellite imagery. (Source: http://www.nasa.gov).

1.2 Problem Statement

Aerosols such as sulfur compounds resulted from emissions by fuel burning and other industrial processes. They are typically found at the lowest three to four kilometres above the earth's surface. It precipitates out of the atmosphere typically in about a week because of its physical nature that could only remain shortly in atmosphere. Because of this short residence time, aerosols become highly variable as a function of location and time. This characteristic has made measuring the aerosol concentration as a big challenge.

Aerosol composition varies with respect to the geographical distribution. The highest concentration are usually found in urban areas, reaching up to 10^8 and 10^9 per cc. Conventional techniques to measure aerosol composition are only covered in a small areas. Accurate retrievals of aerosol concentration, size distribution, optical properties in its spatial also temporal variability over land surfaces from surface based, aircraft and space-based measurements remain a difficult problem.

Large uncertainty in the aerosol forcing of climate needs to be resolved to improve accuracy in predicting future climate change. Aerosol also affected the mankind by changing the radiation balance of the earth and consequently causing health problems of respiratory ducts. Hence, it is desirable to obtain information on aerosol properties. By using remote sensing technique, aerosol concentrations are measured frequently by the temporal resolution of the satellite. A large area is available to be observed by remote sensing instead of conventional technique which covered a small area in specific location.

1.3 Objectives

Objectives of the study are divided into two:

i. To define the sensitivity of NOAA AVHRR data on land tropospheric aerosol, and
ii. To analyse land tropospheric aerosol concentration and distribution over Malaysian environment using NOAA AVHRR.

1.4 Scopes

The limitations in this study are:

i. Tropospheric aerosol over land are extracted from radiance value of NOAA AVHRR imagery which covered Malaysian area.
ii. Aerosol optical thickness (AOT) are extracted through contrast reduction technique of channel 1 (visible) and channel 4 (thermal).
iii. Tropospheric aerosol concentration are mapped over Malaysian area
iv. The accuracy of the results were tested against PM_{10} (particulate matter less than 10 microns) ground based measurements provided by Alam Sekitar Malaysia Berhad (ASMA).

1.5 Study Area

The study area is in Malaysia region and located at 2^{o} 30' N and 112^{o} 30' E, as shown in Figure 1.3. It has total of 328 550 km^2 land area. As a develop country, Malaysian economy is almost exclusively driven by industrial activities. In this area, population of 23 522 482 people continue to grow at a rate of 24% per annum. From the statistics given by Jabatan Pengangkutan Jalan (2005), there are 12 021 929 vehicles on the road in this country which contributed to fossil and fuel burning everyday. With rapid urbanization and industrialization rate, the establishment of aerosol monitoring system is on demand in this area.

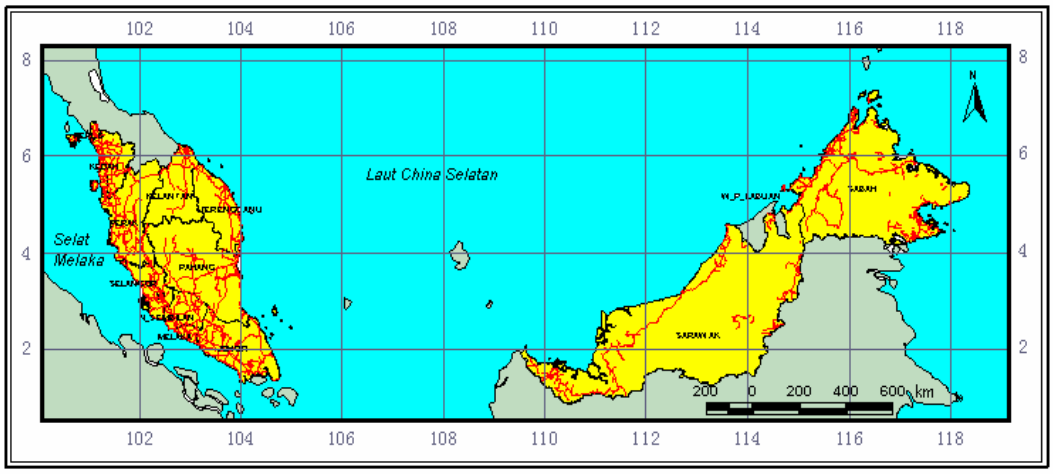

Figure 1.3: Area of study.

1.6 Significance of the study

Aerosol optical thickness measurement is a very important task for monitoring the quality of atmosphere. Various of technique can be used to extract the measurement, but priority is given to the easiest, fastest and low cost method. Hence, remote sensing is the first option to used along with the advance technology in this new millennium.

Aerosol particles have an important impact on many biogeochemical processes by serving as the surfaces for speeding chemical reaction (Kaufman). Biomass burning is an important source of organic particles, while in arid and semiarid regions are sources of mineral dust (Pye, 1987). Aerosol particles also play an important role in tropospheric chemistry by serving as the liquid phase that stimulates chemical reaction (Crutzen, 1983). To fully understand these processes, the aerosol characteristics namely spatial and vertical concentration, temporal evolution, size distribution, composition and optical properties, have to be determined at global scale. Only a remote sensing approach based on routine analysis of satellite data, together with detailed aerosol characterization derived from ground-based stations and in situ instrumentation can supply such needed information.

This research will produce a map that will help the Malaysia Centre for Remote Sensing (MACRES), Malaysia Meteorological Service Department (MMS) and Malaysia Environmental Department in managing Malaysia environment more properly. The result of this study also help Ministry of Health to aware the public on the air quality level in Malaysia.

CHAPTER II

LITERATURE REVIEW

2.1 Introduction

Each year, increasing amounts of aerosol particles are released into the atmosphere due to biomass burning, forest fires, dust storms, volcanic activity, urban and industrial pollution (Figure 2.1). Indeed, biomass burning is a major source of aerosol particles (Crutzen et al. 1985, Andreae et al. 1988).

Aerosol could only remain shortly of time in atmosphere, but the direct and indirect effects of smoke aerosol is comparable to that of sulphate aerosol and may add up globally to a cooling effect as large as $2Wm^{-2}$ (Penner et al., 1992).

Figure 2.1: Industrial pollution and fossil burning from vehicle contribute to high aerosol concentration in the atmosphere.

Satellite remote sensing for aerosol optical thickness (AOT) studies has a history of about 20 years. The major objective of these remote sensing sensors is to study the aerosol effect on global climate change. The information of some major satellite remote sensing applicable for tropospheric aerosol studies are listed in Table 2.1.

Table 2.1: Present remote sensing satellite applicable for remote sensing tropospheric aerosol.

Sensor	**Launching year**	**Spectral channels (μm)**	**Pixel size (km^2)**	**Remote sensing application**
TOMS-Nimbus 7	1978	2 bands (0.34; 0.38)	1.00 x 1.00	Presence of absorbing aerosols
AVHRR	1979	4 bands (0.64; 0.83; 3.75; 11.5)	1.00 x 1.00 or 4.00 x 4.00	Operational remote sensing of AOT over oceans; Angstrom coefficient over ocean. AOT over land using dense vegetation or contrast effects.
Landsat-TM	1982	6 bands (0.47-2.20)	0.03 x 0.03	AOT over oceans; AOT of dust over land using contrast effect.
Landsat MSS	1971	4 bands (0.55-0.90)	0.08 x 0.08	AOT and Angstrom coefficient.
POLDER-ADEOS	1996	8 bands (0.41-0.91) -3 polarized bands -multi-view angles	6.00 x 7.00	AOT, Angstrom coefficient and aerosol model.
SeaWiFS	1997	8 bands (0.41-0.86)	1.00 x 1.00	AOT and Angstrom coefficient over ocean
MODIS	1999	12 bands (0.41-2.10, 3.96)	0.25 x 0.25 or 1.00 x 1.00	AOT and size distribution over ocean, AOT over land.
MISR	1999	4 bands (0.47-0.86)	0.25 x 0.25 or 1.00 x 1.00	AOT, size distribution and phase function over water; AOT over land.

AOT = Aerosol of thickness

2.2 Conceptualization of Aerosol Retrieval

The methods for aerosol retrieval are based on concentration of atmospheric aerosols, or in other word the aerosol optical thickness, τ, from radiance taken from the satellite image itself (Tanre et al., 1992), described by:

$$L(\tau_a, \mu_s, \mu_v, \Phi) = L_o(\tau_a, \mu_s, \mu_v, \Phi) + F_d(\tau_a, \mu_s)T(\tau_a, \mu_v)\rho/[1-s(\tau_a)\rho] \quad \ldots (2.1)$$

where;
L = radiance
L_o = atmospheric path radiance
τ = aerosol optical thickness (AOT)
μ_s = satellite zenith illumination
μ_v = viewing zenith illumination
Φ = azimuth illumination
F_d = downward flux
T = upward transmission
ρ = surface reflectance
s = spherical albedo

From algorithm (2.1), the atmospheric effect is composed of two parts, namely the atmospheric path radiance, L_o, due to photons scattered by the atmosphere to the sensor without being reflected by the surface, and the atmospheric effect on the transmission of the downward flux, F_d, and the upward transmission, T. μ_s, μ_v, Φ describes the zenith illumination, viewing and azimuthal conditions respectively. $[1-s(\tau_a)\rho]$ describes the multiple interaction between the ground and atmosphere where $s(\tau_a)$ is the spherical albedo and ρ is the surface reflectance. Both of the atmospheric effects were used in the past to determine the aerosol optical thickness and reviewed as below.

2.3 Determination of the Aerosol Optical Thickness Using the Path Radiance

In order to determine the aerosol optical thickness from the path radiance, the second term in algorithm (2.1) most be small, so that the uncertainty in the surface reflectance, ρ, will have a minimal effect on the aerosol determination of aerosol. The method was applied over dark surfaces such as oceans and inland water bodies (Griggs, 1975).

Accuracy of the aerosol optical thickness determination by path radiance depends on the accuracy of assumed reflectance on dark objects and the ability to estimate the aerosol scattering phase function and single scattering albedo. The method can be applied to satellite imagery for which it is a priori known that densed vegetation are present, accounting on its geographic location and occurrence season in which the image was taken.

2.4 Determination Based on Atmospheric Transmission (Contrast Reduction)

Determination of aerosol optical thickness from atmospheric transmission is based on ratio of transmission between several images and it is known as contrast reduction. Tanre (1988) has suggested and applied the method TM images taken over arid region. The variation in the transmission is determined from the variation of the difference between radiance from pixels located a specified distance apart. The contrast reduction expressed by

$$\Delta L^*_{ij}(\tau_a, \mu_s, \mu_v) \approx \Delta \rho_{ij} \quad \frac{T(\tau_a, \mu_v) F_d(\tau_a, \mu_s)}{1.-<\rho> s(\tau_a) . 2} \qquad \ldots (2.2)$$

where;

ΔL^*_{ij} = the difference of apparent radiance between two adjacent pixels (i,j) and (i,j+1)

τ = aerosol optical thickness

μ_s = satellite zenith illumination

μ_v = viewing zenith illumination

$\Delta \rho_{ij}$ = actual ground reflectance difference

T = upward transmission

ρ = surface reflectance

s = spherical albedo

F_d = downward flux

ΔL^*_{ij} the represent difference of apparent radiance between two adjacent pixels (i,j) and (i,j+1), where i and j are the geographical coordinates, expressed in line and column number which is related to the actual ground reflectance difference, $\Delta \rho_{ij}$. While ρ is the mean reflectance of the two pixels. $\Delta \rho_{ij}$ and optical thickness can be derived when algorithm (2.2) is applied to a collection of image that includes a relatively clear image. Derivation of optical thickness is independent aerosol scattering phase function, but it is depend on the single scattering albedo, ω_0, and asymmetry parameter of the aerosol.

To express the contrast character the target. ($\Delta \rho_{ij}$), structure function concept, *Fs(d)* is defined by

$$Fs(d)^2 = \frac{1}{n * (m-d)} \sum_{i=1} \sum_{j=1} (\rho_{ij} - \rho_{ij+d})^2 \qquad \ldots (2.3)$$

where;

d = distance between two pixels

$n * (m-d)$ = total number of pixels within the target

ρ_{ij} = actual ground reflectance

d is the distance between two pixels and *n * (m-d)* is the total number of pixels within the target in composing structure function *F*s(d)*. The structure function in satellite observation is *F*s(d)* and the actual structure of the surface *Fs(d)* are related by

$$F^*s(d) \approx Fs(d) \frac{T(\tau_a, \mu_v) F_d(\tau_a, \mu_s)}{1 - A * s(\tau_a)} \quad \ldots (2.4)$$

where;

A = mean albedo of the target

As provided that *Fs(d)* is known and invariant, the satellite measurements allow us to estimate the aerosol optical thickness by means of the transmissions functions of (2.4).

2.5 Derivation of Aerosol

Initially, distribution of aerosol always been monitored from ground-based station. Many programmes have been developed in local and global scale. These programmes provide aerosol monitoring services a well as validate the satellite measurements.

Aerosol measurements began at the Climate Monitoring and Diagnostic Laboratory (CMDL) baseline observatory in the mid-1970's apart of the Geophysical Monitoring for Climate Change (GMCC) program. Since the inception of the program, scientific understanding on the behavior of atmospheric aerosols has improved considerably. One lesson has learned is that human activities primarily moreinfluence

aerosols in regional and continental scales rather than global scales. The goals of regional-scale monitoring program are to characterize means, variability, and trends of climate-forcing properties in different types of aerosols, and to understand the factors that control these properties. CMDL's measurements also provide ground-truth observation for satellite measurements and global models, as well as dominant aerosol parameters for global-scale models. CMDL has various ground control station distribute across the European region.

The Aerosol Robotic Network (AERONET) program is an inclusive federation of ground-based remote sensing aerosol networks established by multi agency that are related to aerosol studies. This program is distributed at hundred of stations around the world purposely for monitoring global aerosol behaviour as shown in Figure 2.2. Their goals are to assess aerosol optical properties and validate the network imposes standard on instrument installation, sensor calibration and data processing. In this collaboration, data of spectral aerosol optical depth and perceptible water and collected globally in diverse aerosol regimes.

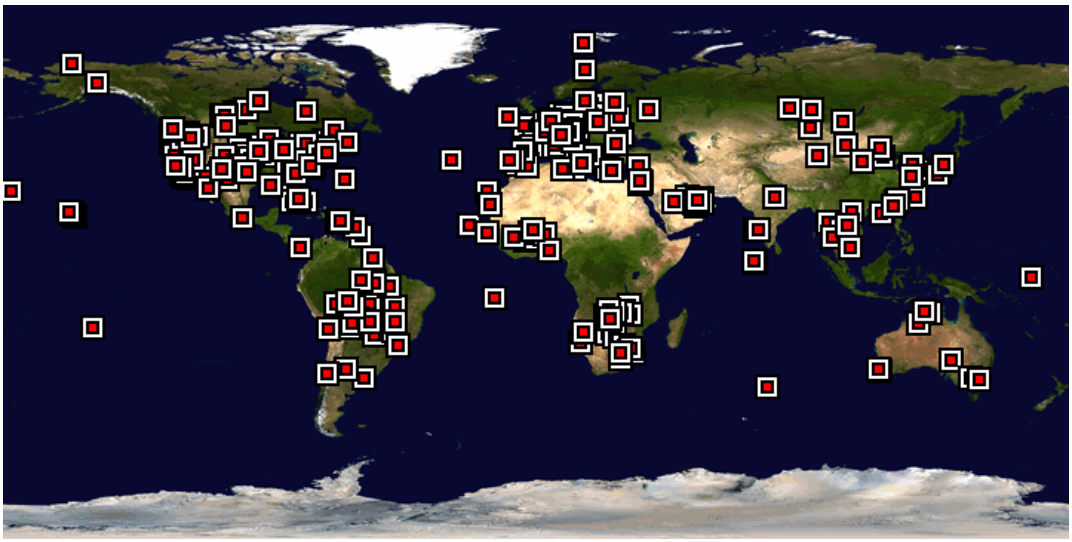

Figure 2.2: Distribution of AERONET station.

2.6 Aerosol Retrieval Using Remote Sensing

Decoupling the atmospheric effects such as water vapour, ozone absorption, aerosol and molecular scattering from the terrestrial surface signal have been fairly andsuccessfully achieved (Tanre et al., 1992). Unlike all, aerosols can be distinguished accurately from ancillary data sources and used for satellite correction. This has led to the development of aerosol retrieval in which the radiance from over ocean is inverted to an appropriate aerosol model for obtaining the correct aerosol optical thickness at such surface reflectance.

Aerosol remote sensing was developed using a single wavelength and single angle of observation (Kaufman et al., 2002). TOMS (Total Ozone Mapping Spectrometer) has flown since 1978, and it two channels that are sensitive to ultraviolet light that were discovered to be excellent for observation of elevated smoke or dust layers above scattering atmosphere observation. TOMS is among the first instrument to allow observation of aerosols as the particles always spread across the land and sea boundary. From TOMS data as in Figure 2.3, it is possible to observe a wide range of phenomena such as desert dust storms, forest fires and biomass burning.

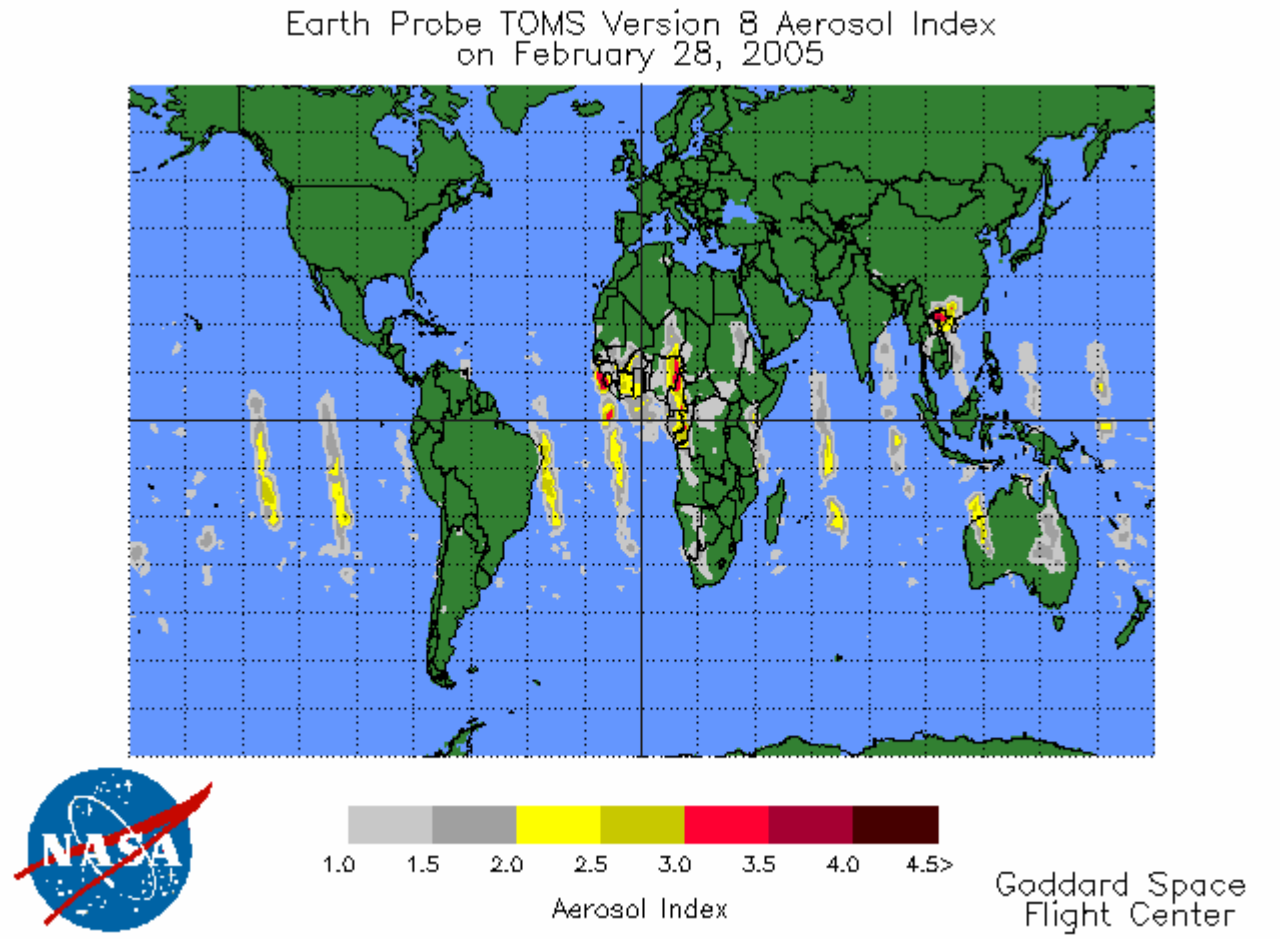

Figure 2.3: Aerosol condition from Earth Probe TOMS on 8 February 2005.

One of the first instrument designed for aerosol measurements is POLDER (Polarization and Directionality of the Earth's Reflectances). It relies on spectral channels in a range wider than human vision ability (0.44 - 0.86μm). The instrument comprises a wide-angle camera that observes similar target on the earth at different angles and up to zenith angle of 65^{o}. POLDER also measures light polarization to detect fine aerosols over land, taking advantage of the difference between the spectrally neutral polarized light reflected from the earth's surface and the spectrally decreasing polarized light reflected by fine aerosols.

Virtually, all procedures for retrieving aerosols from satellite data over land areas require a priori knowledge of the surface and require a change detection procedure (Holben et al., 1992). Typically, these have been developed using high resolution Landsat and SPOT data. A complimentary technique was developed using TM data (Figure 2.4) which selects invariant targets and relates the change in contrast between the invariant targets to the aerosol optical thickness on a reference day (Sifakis et al., 1988). In a more simplified approach, in term of brightness method, the apparent changes in reflectance above a pixel from one day to another is related to the difference in optical thickness between the two days assuming the surface reflectance did not has changes.

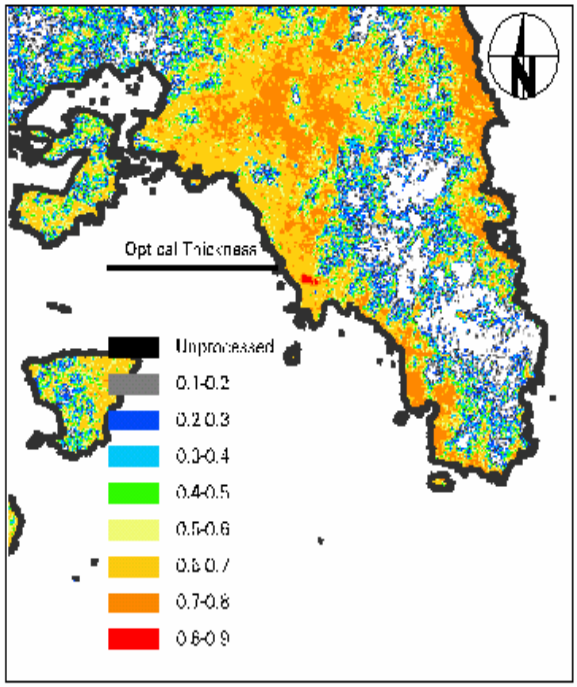

Figure 2.4: Aerosol optical thickness derived from Landsat TM over Athens using contrast reduction approach (source: Sifiakis et al., 2002)

Two instruments, MODIS (Moderate Resolution Imaging Spectroradiometer) and MISR (Multi-angle Imaging Spectroradiometer) on the Terra satellite have measured global aerosol concentrations and properties since 2000. MODIS measures aerosol optical thickness over land with an estimated error of ± 0.05 to ± 0.20 (Kaufman et al.,

2002). In land application, MODIS uses the 2.1μm channel to observe surface cover properties, estimate surface reflectance at visible wavelength and derive aerosol optical thickness from the residual reflectance at the top of atmosphere.

The amount of light penetrating the top of atmosphere is affected by the angle where the light was reflected by the surface or atmosphere. MISR took advantage of this fact by detecting the reflected light at different viewing angles (nadir 70^{o} in forward and backward motion) along the satellite's track in a narrow spectral range (0.44-0.86μm). It is thus able to separate the aerosol signal from that of surface reflectance and then determine the aerosol properties. A mixed approach using two viewing directions but in a wider spectral range (0.55-1.65μm) is used by ATSR (Along Track Scanning Radiometer) to derive the aerosol concentration and type.

Over bright desert, the magnitude of dust absorption is determined if dust has brightens or darkens the image. This property is very useful to estimate the aerosol optical thickness. Such satellite measurements, in agreement with *in situ*, aircraft and radiation network measurement of dust absorption, helped to solve a long standing uncertainty in desert dust absorption of sunlight.

Advanced Very High Resolution Radiometer (AVHRR) instrument has been used by numerous researches to detect aerosol optical thickness over land and oceans (e.g., Stowe et. al., 1997, Husar et. al., 1997, Hindman et. al., 1984, Paronis and Sifakis, 2003). Unlike the nearest satellite sensors, AVHRR enables to provide a temporal coverage which is not accessible since the past twenty years.

Atmospheric effect in NOAA depends on the position of spectral bands and instantaneous field of view (IFOV) of the instrument. Sifakis et al. (2003) has studied the

potentiality of using NOAA-15 observations for obtaining AOT maps over the metropolitan area of Athens through Differential Textural Analysis (DTA) algorithm. The result from this study is presented in Figure 2.5. Correlation as high as 0.78 to 0.95 are retrieved between the AOT values and PM_{10} measurements.

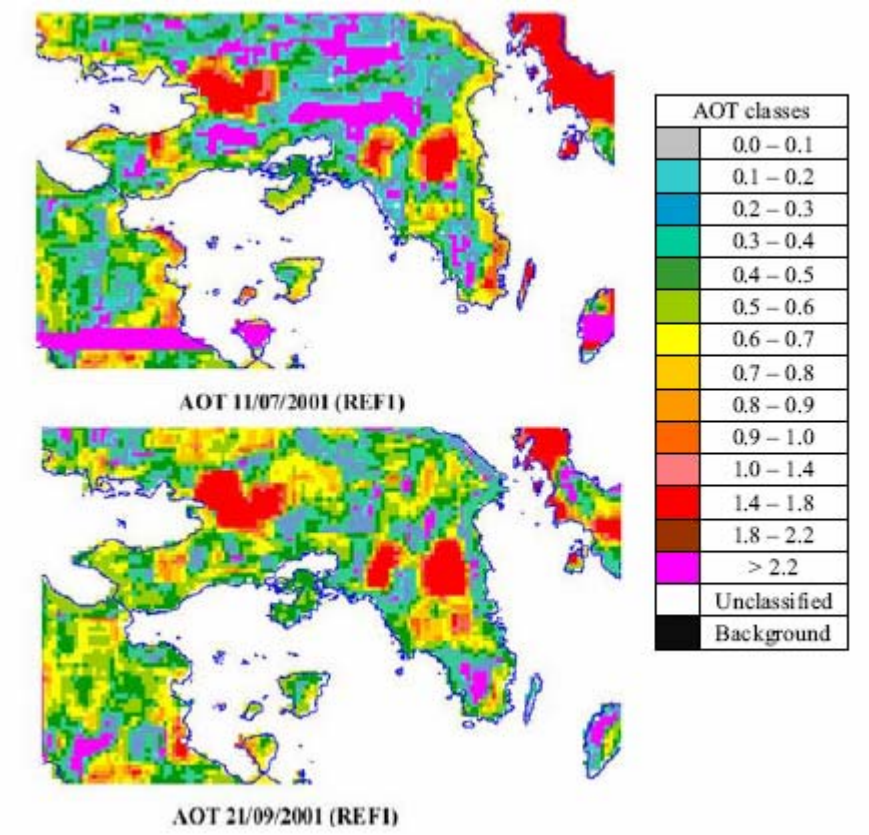

Figure 2.5: AOT distribution over Athens from NOAA imagery contrast reduction technique (Sifakis et al., 2002)

CHAPTER 3

METHODOLOGY

3.1 Introduction

In this chapter will discuss about the methodology involved in this study. The methodology is divided into three major parts: data acquisition, data pre-processing and data processing. In this study, a pair of NOAA AVHRR (National Oceanic and Atmospheric Administrator Advanced Very High Resolution Radiometer) imagery were represent as fine day data and pollution occurrence data, PM_{10} (particulate matter smaller than 10μm) also used in the processing. In preprocessing radiometric correction, geometric correction and water masking routine were implemented initially on both satellite images

Contrast reduction technique is used in order to extract the aerosol optical thickness (AOT). Contrast reduction technique is divided into two major processing schemes. Differential Textural algorithm is applied to the calibrated channel 1 NOAA data. After that, Thermal Band Difference is applied to thermal channel in order to allow a cross-checking on the results from contrast reduction procedure. Figure 3.1 shows the workflow of the study.

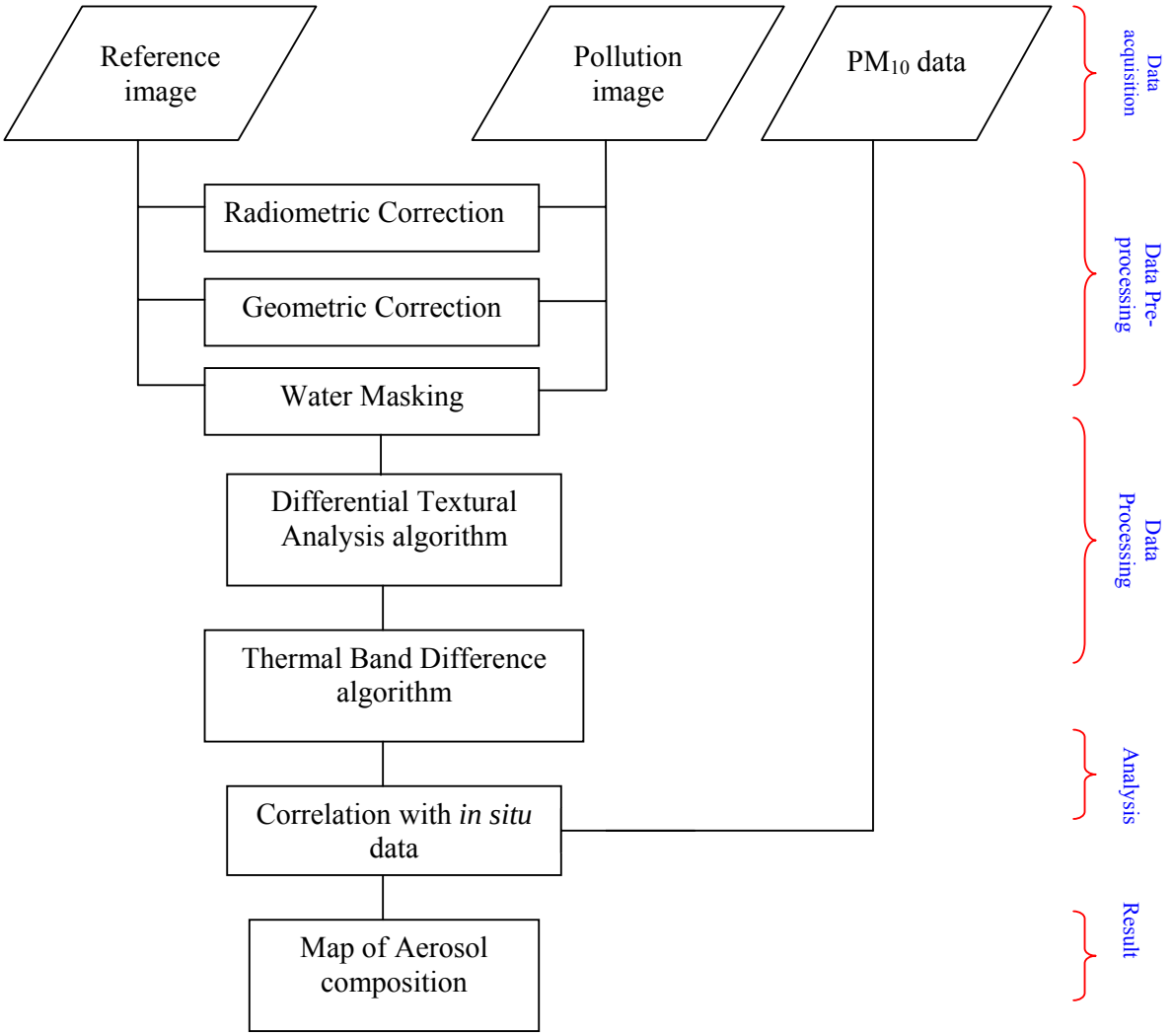

Figure 3.1: Research operational framework.

3.2 Data Collection

A series of NOAA 16 data are used in this study. Each series is composed by:

i. A 'reference image', which is ideally, represented as pollution-free image, and.
ii. A '*pollution image*', which corresponds to a representative or characteristic pollution level.

Data selection is necessary for the reliability of results. Images are selected according to the availability of pollution measurement by a maximum number of monitoring stations and representativeness of the pollution levels recorded by local monitoring networks, or by the standard criteria for image quality and cloud cover. Table 3.1 tabulated the date of three images used as Reference Image in this study. The data are taken from three different dates in years from 2002 to 2004.

Table 3.1: List of data used as Reference Image.

	Reference Data	Date
1	Reference 1	17/05/2002
2	Reference 2	18/06/2003
3	Reference 3	18/05/2004

The data represented polluted day are listed in table 3.2. Both of the reference and polluted data were taken at 3.00 p.m. in local time. These data set are considered suitable for this study by assuming that the atmosphere is stable to active industrial event at data acquisition time.

Table 3.2: List of data used as Polluted Image

	Polluted Data	Date
1	Polluted 1	20/07/2002
2	Polluted 2	08/06/2003
3	Polluted 3	26/05/2004

Accuracy assessment is carried out by taking a collection of in situ data into the processing. In situ data as PM_{10} ground based measurement provided by Alam Sekitar Malaysia Berhad (ASMA). These data were collected at 5 monitoring stations evenly distributed over Peninsular Malaysia namely, Kuala Lumpur (101° 42.274' E, 03° 08.286' N), Prai (100° 24.194’ E, 05° 23.890’ N), Pasir Gudang (103° 53.637' E, 01° 28.225' N), Bukit Rambai (102° 10.554' E, 02° 15.924' N) and Bukit Kuang (103° 25.826' E, 03° 16.260' N).

3.3 Pre-processing

In data pre-processing, three major process namely geometric correction, radiometric correction and masking of water area were applied to the image before further processing is carried out.

3.3.1 Geometric Correction

Firstly, pre-processing started at which the processing concerns the geometrical control on both images. It is proposed to super-impose the images to a topographic map. The images are rectified relatively according to a map projection by with the least-square regression method and resampled relative pixel by the nearest-neighbour algorithm in order to maintain distribution patterns of the pixels and avoid any error on the raw radiometric values. Corrected images were projected to Geographic Lat/Long Projection with Everest (Malaysia and Singapore, 1948) Datum. The reference points used to resample the satellite images were taken from vector layer representing Malaysia boundary. The RMS error for each images are shown in Table 3.3. Generally, the RMS error is lower and considered accurate enough to be used in

further processing. At least 12 to 20 points were used to correct each images in its proper geometry.

Table 3.3: RMS error value for each image.

Images	Control point error in x (pixel)	Control point error in y (pixel)	Total RMS error (pixel)
Reference 1	0.0200	0.0669	0.0698
Reference 2	0.0262	0.0082	0.0275
Reference 3	0.0293	0.0386	0.0484
Polluted 1	0.0170	0.0091	0.0193
Polluted 2	0.0696	0.0271	0.0747
Polluted 3	0.0640	0.1044	0.1224

The effect of geometry correction process is shown in figure 3.2(a) and (b). The corrected imageis shown in figure 3.2 (b) and it has the same coordinate in the real world.

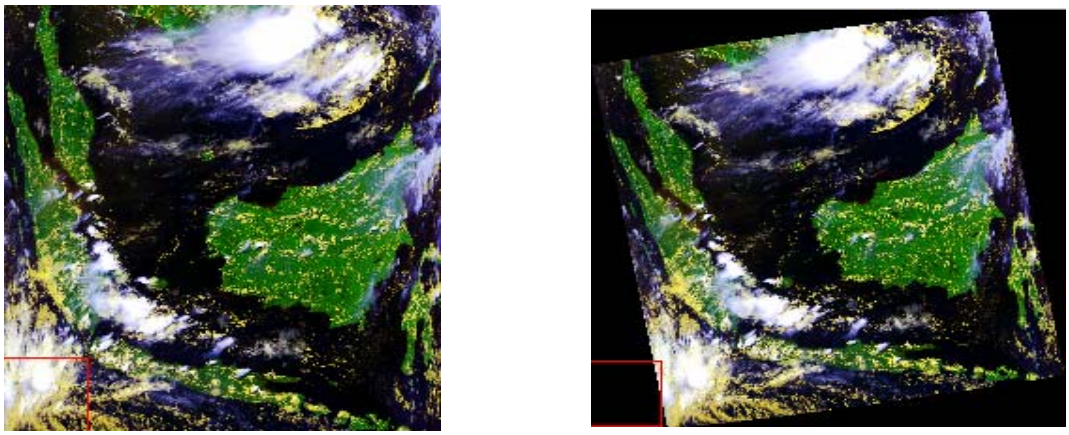

(a) (b)

Figure (3.2): (a) Original NOAA-16 datataken on 18 May 2004 in Channel 1, 2 and 4. (b) Geometrically corrected image.

3.3.2 Radiometric Correction

Radiometric correction is applied by transforming the values of digital number (DN) to radiance or reflectance values through the algorithm as follows:

$$A = S + I \quad \ldots (3.1)$$

where;

A = Reflectance factor or scale of radiance (albedo)

S = Slope value

I = Intercept value

The result of radiometrically corrected process is shown in figure 3.3.

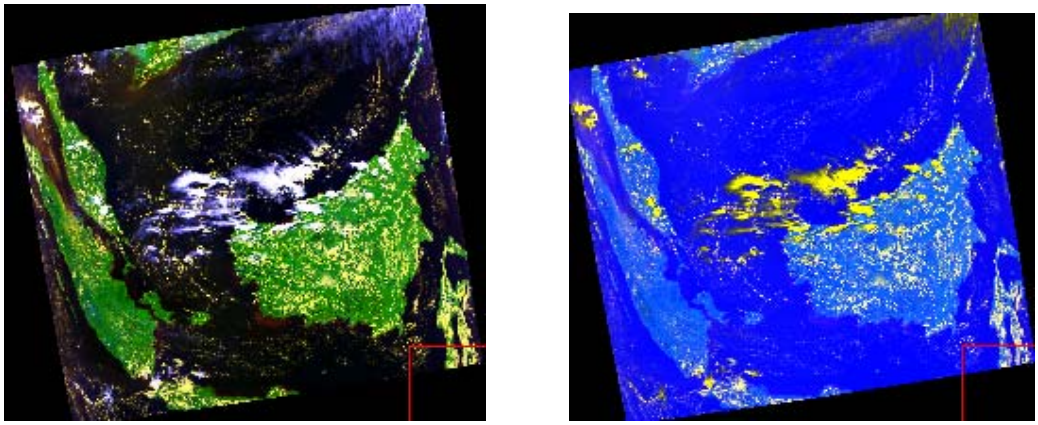

(a) (b)

Figure 3.3: (a) Geometrically corrected image. (b) Calibrated image.

3.3.3 Masking Out Water Bodies

Masking image is an image with two representating the land area and water surface. In order to extract aerosol information over land area, all the information

related to sea surface and water bodies must be isolated and excluded out from the calibrated images, as in figure 3.4 (a). This study area is consisted of 328 550 km^2 of land area and 1 200 km^2 of water area. Water bodies were found along South China Sea and Straits of Malacca as well as within lake, river and other water bodies as shown in figure 3.4 (b). This process is applied to each image used in the study.

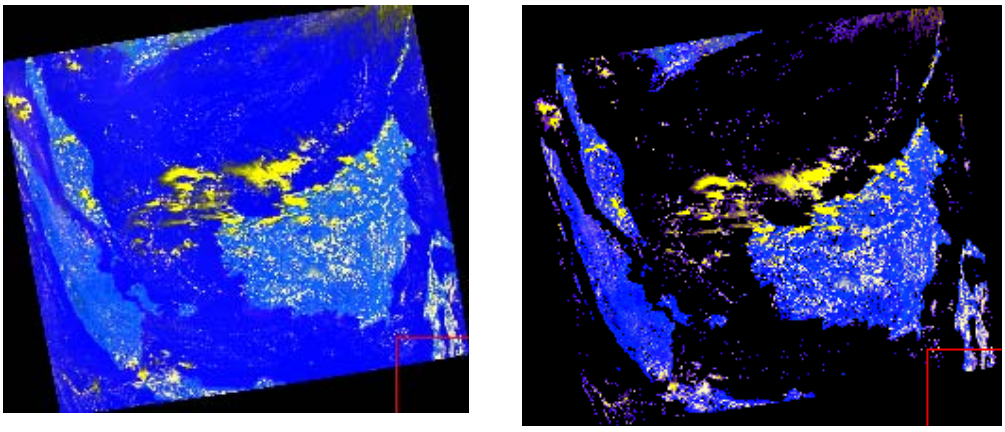

(a) (b)

Figure 3.4: (a) Calibrated NOAA data. (b) Masked of water images.

3.4 Satellite Data Processing

After pre-processing procedure, further processing is applied in order to extract aerosol optical thickness distribution over land area. The processing, namely contrast reduction maps the AOT by comparing the fine day data with polluted day data. Contrast reduction is carried out by performing Differential Textural Analysis (DTA) and temperature attenuation procedure on channel 1and 4 calibrated of NOAA data, respectively.

3.4.1 Differential Textural Analysis (DTA)

Differential Textural Analysis (DTA) uses two images namely a 'Reference' and a 'Polluted' image that have been acquired on a low pollution and a high pollution day. The underlying surface between the two acquisition images must be relatively unchanged and taken in same observation geometry. Hence, it has minimized the uncertainties due to both the seasonal variations of the ground reflectance and the surface bi-directionality effect (Paronis and Sifakis, 2003).

The main part of DTA calculates the local standard deviation of radiance in both images as follows:

$$\sigma = \sqrt{\left[\frac{\Sigma (\rho - \mu)^2}{n} \right]} \qquad \ldots (3.2)$$

Where;

σ = Local standard deviation of radiance values

ρ = Radiance of Channel 1

μ = Local mean of radiance values

n = pixels of 3x3 local window

Sifakis et al (2003) used 7 x 7 pixels window to measure out the standard deviation due to availability of huge number of ground-based data. Therefore, it is sufficient enough to used 3 x 3 pixels window in small number of ground-based data. The result presented in figure 3.5.

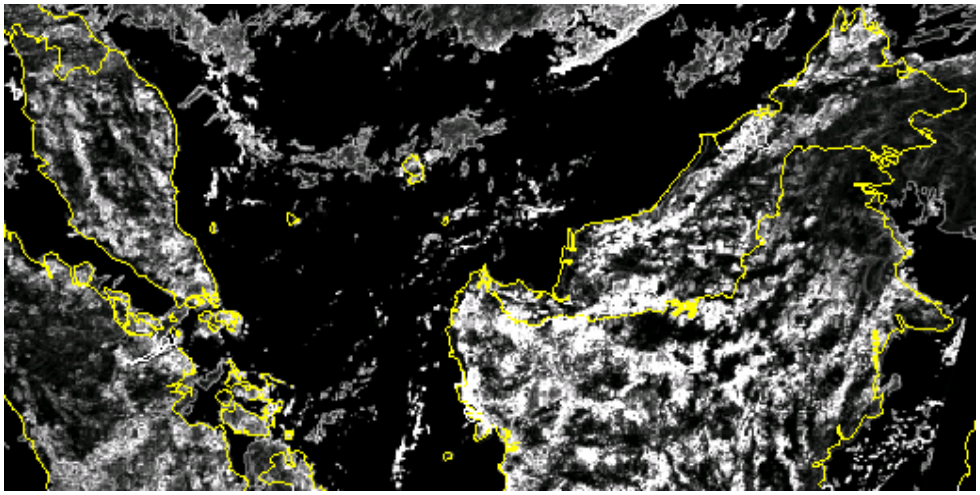

Figure 3.5 : Local standard deviation image from 3x3 windows .

The presence aerosol layer in the atmosphere has reducing effect in image contrast. The contrast reduction is directly related to the optical thickness of the layer (Tanre *et al.* , 1993). The ratio of contrast between two different day images on two different days is expressed as:

$$\tau = \ln\left[\frac{\sigma(\rho_{reference})}{\sigma(\rho_{pollution})}\right] \quad \ldots (3.3)$$

where;

τ = optical thickness values

σ = Local standard deviation of radiance values

$\rho_{reference}$ = radiance values of Channel 1of reference image

$\rho_{pollution}$ = radiance values of Channel 1of pollution image

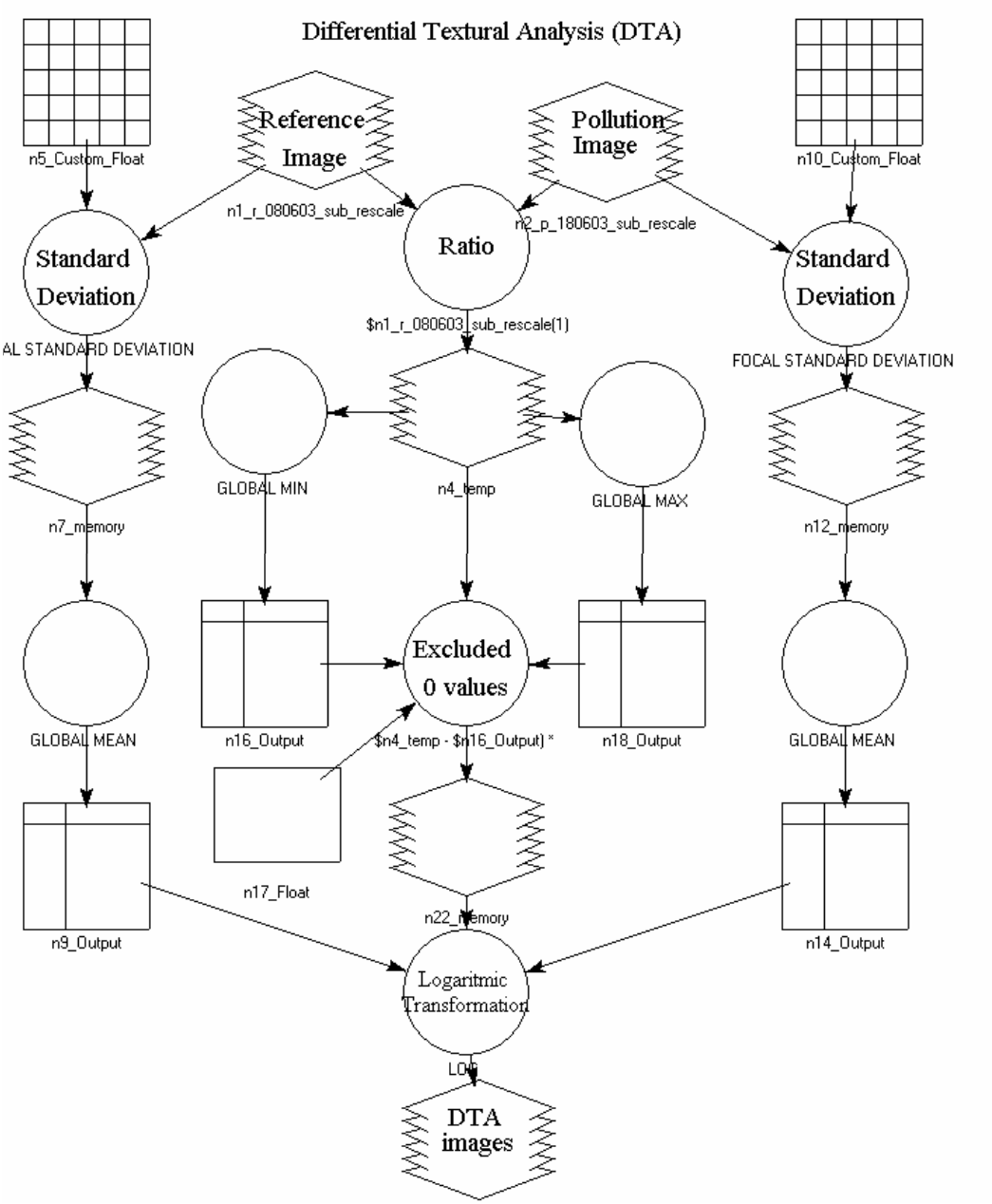

Figure 3.6: Structure of DTA model.

In order to cross-checking on the result, temperature attenuation procedure is applied to the reference and pollution image by maintaining only land areas from calibration of thermal band. Thermal band values are converted to radiance by formula of:

$$N_E = a_0 + a_1 C_E + a_2 C_E^2 \quad \ldots (3.4)$$

where;

N_E = radiance value in mW/(m_2-sr -cm_{-1})

a_0, a_1, a_2 = thermal operational coefficient of channel 4

C_E = DN value of channel 4

To convert radiance value into an equivalent blackbody temperature, two processing steps as follows have to be defined

$$T_E^* = \frac{C_2 V_c}{\ln\left(1 + \left(\frac{C_1 V_c^3}{N_E}\right)\right)} \quad . (3.5)$$

$$T_E = \frac{T_E^* - A}{B} \quad \ldots (3.6)$$

where;

T_E = Equivalent blackbody temperature

$C_1 = 1.1910427 \times 10^{-5}$ mW/(m_2 -sr-cm_{-4})

C_2 = 1.4387752 cm-K

V_c = 917.2289 (for NOAA-16)

A = 0.332380 (for NOAA-16)

B = 0.998522 (for NOAA-16)

Temperature attenuation is applied to estimate the observed relative temperature variation with the result shown in Figure (3.7). TBDF or thermal band difference are carried out through the following algorithm

$$TBDF = (T_{E\ reference}) - (T_{E\ pollution}) \quad \ldots (3.7)$$

where;

$T_{E\ reference}$ = Equivalent blackbody temperature for reference image

$T_{E\ pollution}$ = Equivalent blackbody temperature for polluted image

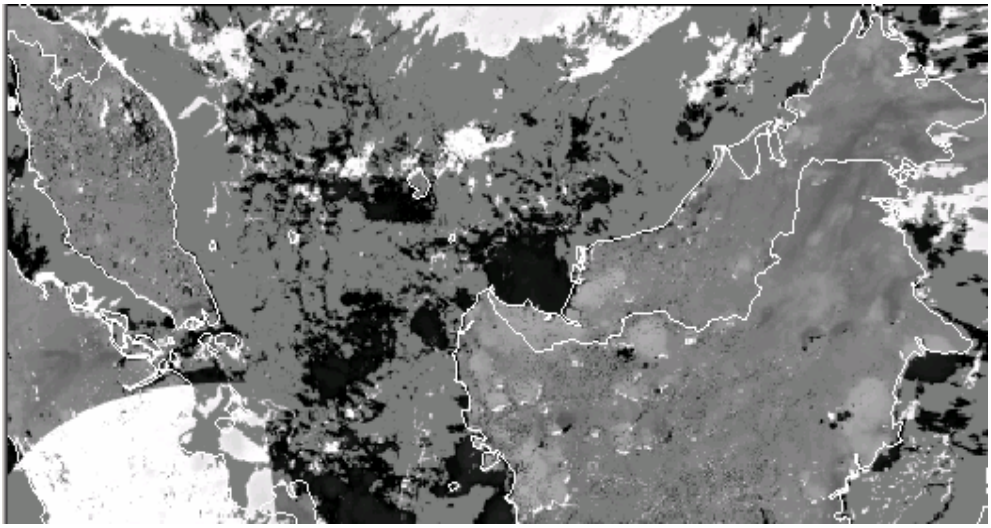

Figure 3.7: Thermal band difference image of Reference 3 and Polluted 3 images.

Finally, information related to water bodies are excluded from the result cross-checking the DTA images and TBDF images. DTA images that have TBDF value lower than 1 are replaced by 0.

CHAPTER IV

RESULT AND ANALYSIS

4.1 Introduction

This chapter discussed and analyzed the output obtained through this study. The discussions are divided into final map analysis and regression analysis from correlation graph.

4.2 Aerosol Optical Thickness (AOT) Distribution From NOAA-16

Figure 4.1 shows the distribution of aerosol optical thickness (AOT) over land of Malaysia on 20/07/2002. It is shown clearly by the figure that the AOT value over Malaysia are low. It should be noted that ‘Unclassified’ pixels over the northern part of Peninsular Malaysia were due to the presence of cloud appearing in Reference 1 image. This situation is consequent to cloud presence in the reference images, indicating the importance of choosing the appropriate cloud-free reference images. Aerosols concentration are indicated through the colour of red for high AOT value and blue for low AOT value.

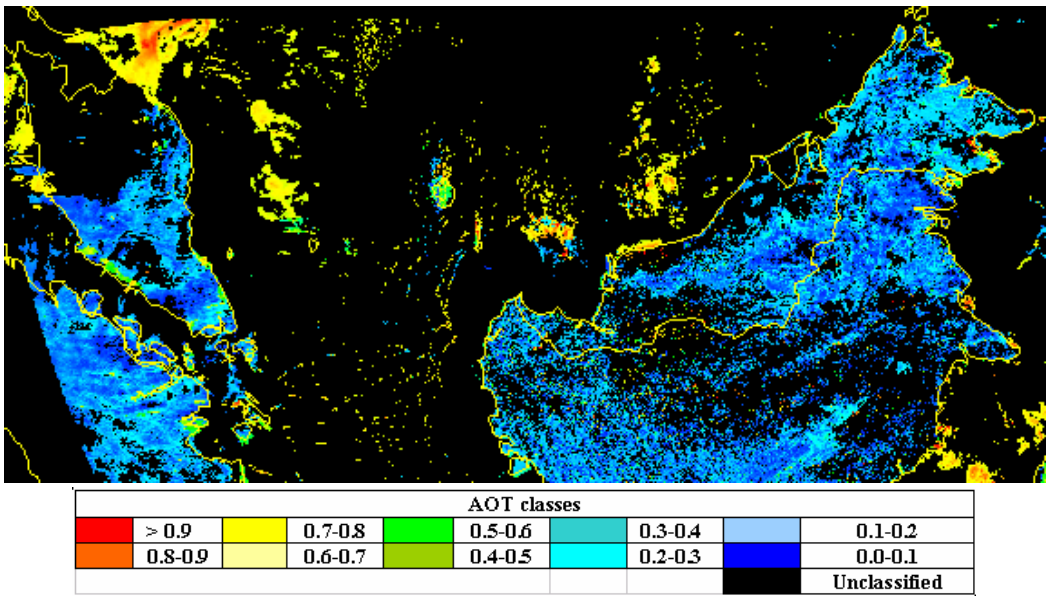

Figure 4.1: AOT maps derived from 'Reference' and 'Polluted' images of 17/05/2002 and 20/07/2002, respectively

Pixels distribution is shown in Figure 4.2. The pie chart show that 75% of the pixels in the image are represent 'Unclassified' pixels. This is due to the presence a lot of cloud especially in the Reference 1 image. The cloud can be identified in almost half of Peninsular Malaysia area. The 'Unclassified' pixel also represent water body area whish is cover almost 60% of the study area. The highest concentration of AOT indicated by red colour represent 1573 pixels from the whole image. This red pixel can be found in Pulau Borneo and Johor Bahru. While the lowest AOT values indicate by dark blue in colour is represent 11% of the pixels from the image.

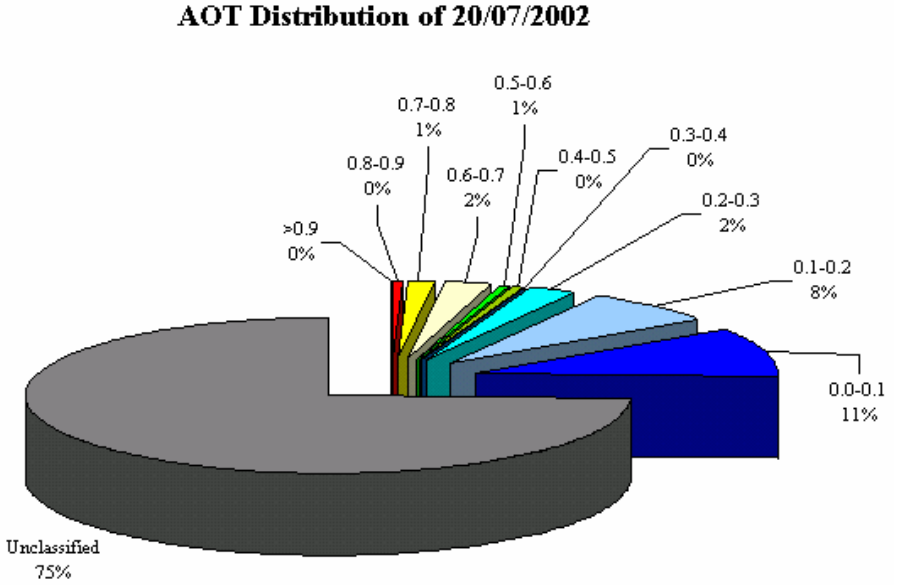

Figure 4.2: Partition of AOT value on 20/07/2002.

Figure 4.3 shows the distribution of aerosol optical thickness (AOT) over land of Malaysia derived on 18/06/2003. Aerosols concentration are indicated through temperature aggregation which the colour of red for high AOT value while blue for low AOT value. It is shown clearly by the figure that the AOT value over Malaysia are low. High AOT value can be found in Pulau Pinang, along West Peninsular Malaysia, Johor Bahru, Singapore and some places in Sarawak. Most of this places are industrial and high population area.

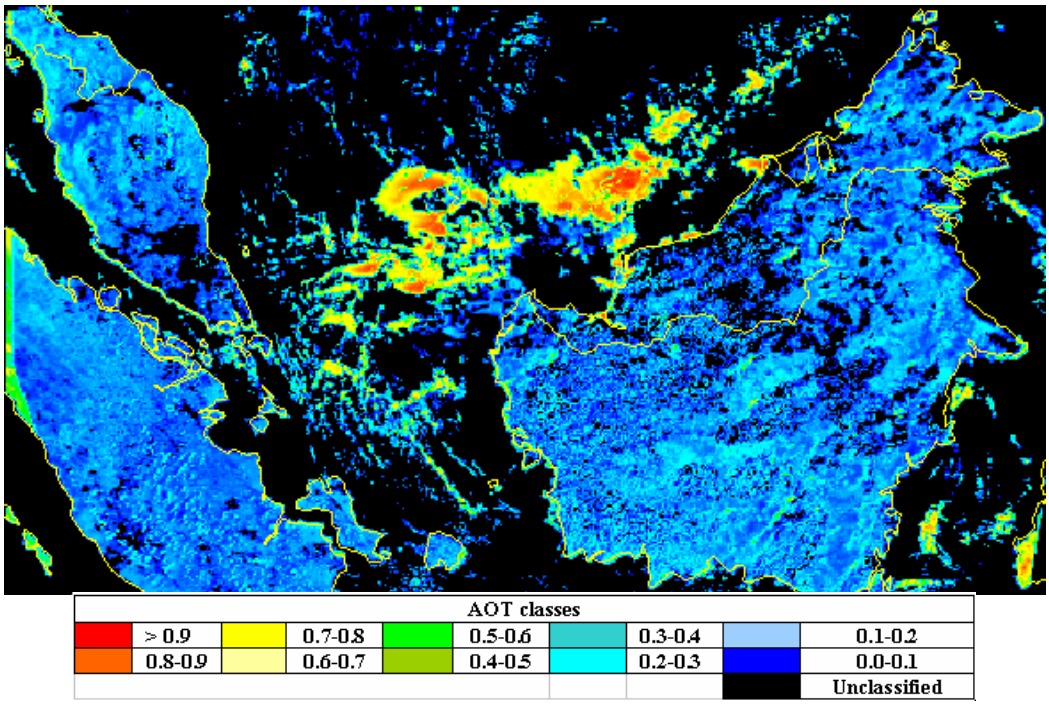

Figure 4.3: AOT maps derived from ‘Reference’ and ‘Polluted’ images of 08/06/2003 and 18/06/2003, respectively.

Figure (4.4), show a pie chart with the percent distribution of AOT pixels. The aerosol distribution over Malaysia on 18/06/2003 are higher compare to Figure (4.1). 1% of the region gain a high aerosol measurement which is represent 11368 pixels from total of 2226560 pixels per image.

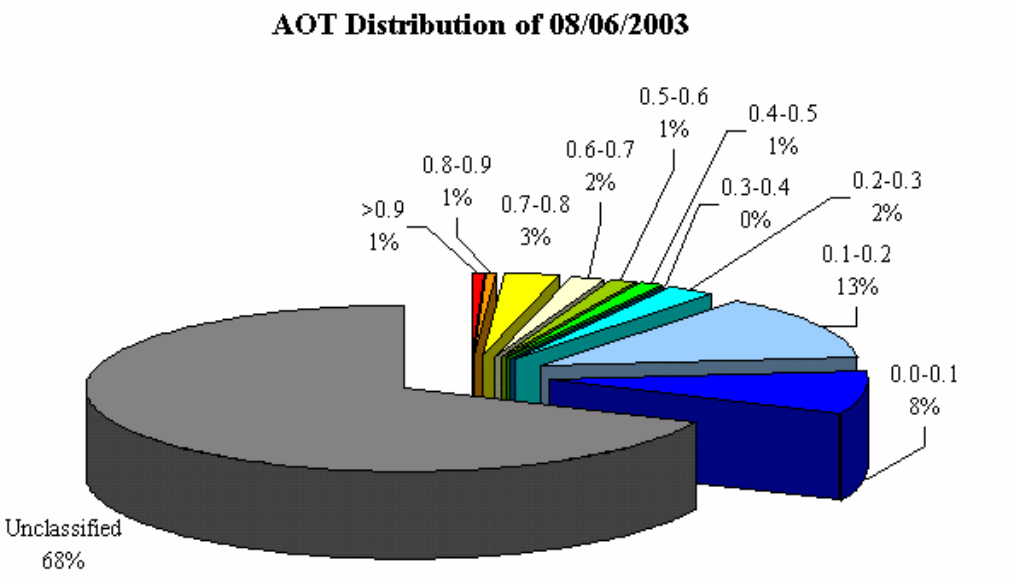

Figure 4.4: Partition of AOT distribution derived on 08/06/2003.

The DTA algorithm applied on a series of AVHRR data over Malaysia region. From the study, aerosol distribution over Malaysia on 26/05/2004 (as shown in Figure 4.5) is relatively low. Only Penang shows a high value of AOT. Some places with high population, namely Kuala Lumpur and Johor Bahru also gain high aerosol concentration.

High AOT values (depicted in red) over sea area were due to the presence of clouds appearing and has to be ignored because the algorithm used in this study is only valid for extraction of AOT value over land and not effective for water surface.

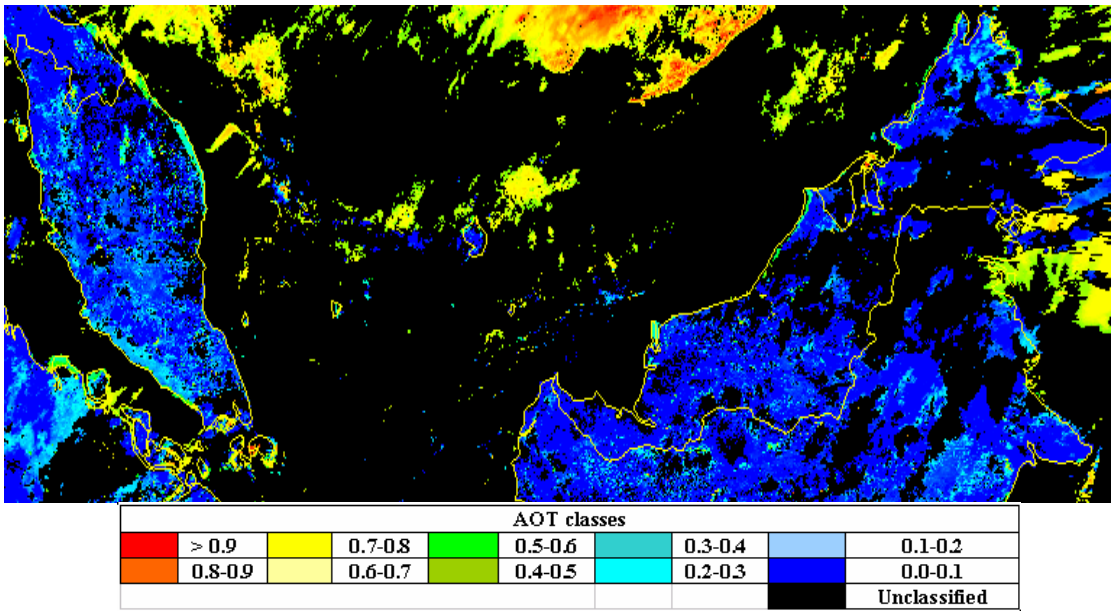

Figure 4.5: AOT maps derived from 'Reference' and 'Polluted' images of 18/05/2004 and 26/05/2004, respectively.

AOT distribution derived from 26/05/2004 is shown in Figure 4.6. The pie chart show that 83% of the pixels in the image are represent 'Unclassified' pixels. 'Unclassified' pixels are covered cloud and water area. The highest concentration of AOT indicated by red colour represent 2535 pixels from the whole image.

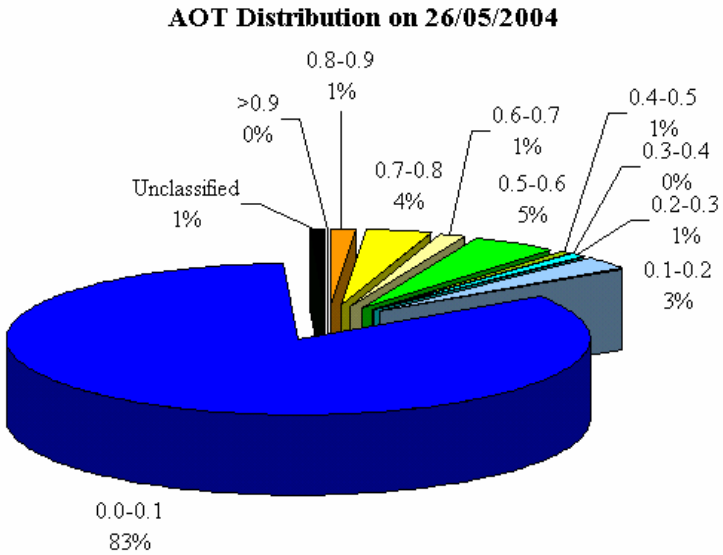

Figure 4.6: Partition of AOT distribution derived on 26/05/2004.

4.3 Correlation of AOT With PM_{10}

The accuracy of the results was correlated against PM_{10} ground based measurements provided by Alam Sekitar Malaysia Berhad (ASMA). PM_{10} is referred to particulate matter that has a size less than 10 microns. These data were collected at 5 monitoring stations evenly distributed in Malaysia namely, Kuala Lumpur, Prai, Pasir Gudang, Bukit Rambai and Bukit Kuang. The respective scatter plots are presented in Figure 4.7, Figure 4.8 and Figure 4.9.

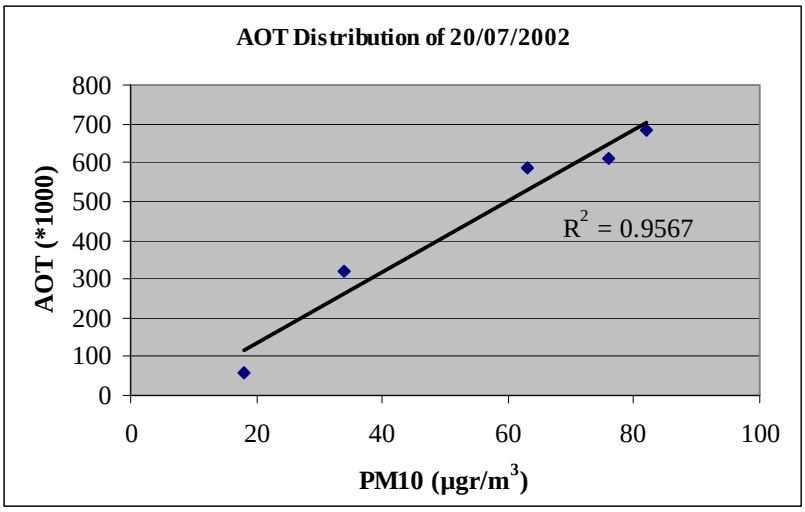

Figure 4.7: Retrieved AOT distribution vs PM_{10} value for 20/07/2004.

All the data reveal a good relationship with PM_{10} measurements where the r^2 is exceeding 0.8. It is noteworthy that the correlation coefficients are high for 2002, 2003 and 2004 (0.9567, 0.8633 and 0.8361, respectively). From the study, Bukit Kuang recorded the lowest aerosol distribution both from the PM10 measurement and AOT retrieval from satellite. This is maybe because it is located in non-urban area. Kuala Lumpur and Pasir Gudang used to gain the highest aerosol measurement.

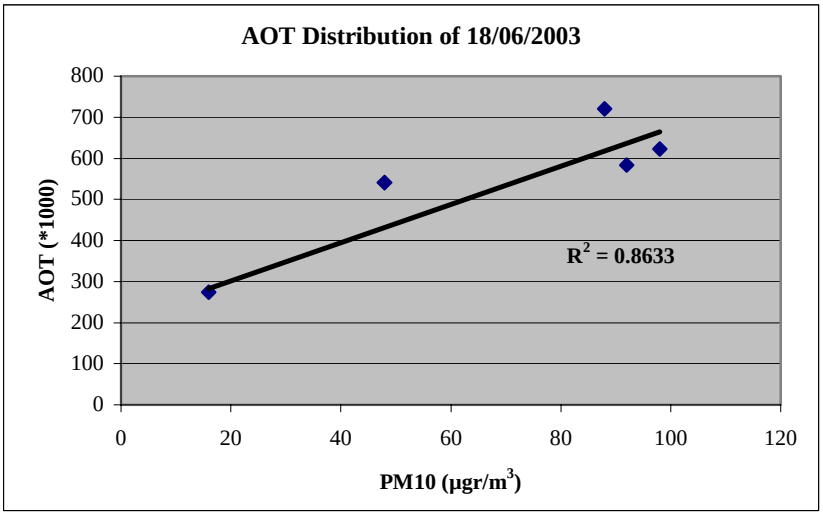

Figure 4.8: Retrieved AOT distribution vs PM_{10} value for 18/06/2003.

This agreement suggests that the application of the DTA algorithm on NOAA-16 AVHRR images whenever available and cloud free could be used to provide daily AOT maps, depicting air quality information for Malaysia region.

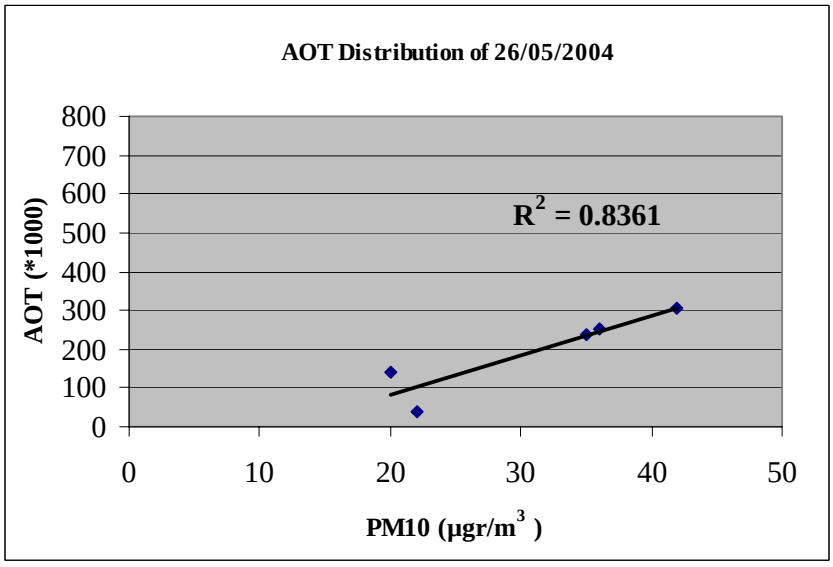

Figure 4.9: Retrieved AOT distribution vs PM_{10} value for 26/05/2004.

CHAPTER V

CONCLUSION

5.1 Conclusion

This research presented the potential of extracting AOT map from low resolution data, NOAA-16 over Malaysia region. The high correlation is found between AOT values and PM_{10} measurement, which suggest that the application of DTA algorithm is best used on available and cloud free AVHRR imagery. In fact, the daily AOT maps indicate air quality information which are somehow minimizing the cost and time compared to the conservative observation.

However, the method is usually restricted due to its low spatial resolution. This could be possibly alleviated by the synergistic ue of high spatial resolution images (i.e Landsat TM and SPOT XS. Cloud presence also could be one of the great limitation for the result reliability a tropical area as Malaysia. Cloud cover is a major problem and in thus limit the accuracy of the results.limitation is a very common problem.

5.2 Recommendation

The dynamic movement of aerosol over land and oceans requires frequent monitoring from the space. In fact the dynamic range and out sources of aerosols are mostly generated from the land. Likely, the remote sensing of aerosol is particularly important to digest human understanding on transformation of aerosol in atmosphere on transformations of aerosol in atmosphere. In comparison, aerosol above the ocean regions is more accurate to be retrieved and much informative due to dark ` and uniform ocean reflectance. Ocean occupies 2/3 of the earth surfaces and naturally interacts with 2/3 of the solar radiation. By relying with remote sensing in routine observation, the behavior of aerosol in the atmosphere could be exposed and consequently, initial prediction of corresponding human activity involved in the aerosol formation will be determine.

The addition of active sensors such as lidar, makes it possible to measure thin aerosol layers which are not easily observed by multispectral scanners. The well calibrated radiometers in conjunction with lidar measurement which observed at the same accuracy of tropospheric aerosol level, particularly in low optical thickness conditions.

Remote observation from space has discovered aerosol in term of its physical and optical properties. The combination spaceborne with ground based measurement permits the observation comprehensive description of aerosol impact on the earth climate. Finally, both measurements are useful to derive the solid aerosol optical properties over the world.

REFRENCES

Andreae, M. O.,Browell, E. V., Garstang, M., Gregory, G. L., Harris,R. C., Hill, G. F., Jaqcob, D. J.,Pereira, M. C., Sachse, G. W., Setzer, A. W., Silva Dias, P. L., Tablot, R. W., Torres, A. L, and Wofsky, S. C., (1988). Biomass burning emissions and associated haze layers over Amazonia. *Journal Geophysical Research*, 93, 1509-1527.

Charlson, R. J., Schwartz, S. E., Hales, J. M., Cess, R. D., Coakley, J. A., Hansen, J. E., and Hoffman, D. J. (1992). Climate Forcing By Anthropogenic Aerosols. *Science*, 255, 423-430.

Cofala, J., Amann, M., Gyarfas, F., Schoepp, W., Boudri, J. C., Hordijk. L., Kroeze, C., Junfeng, L., Dai Lin, Panwar, T. S. and Gupta, S. (2004). Cost-effective Control of SO_2 Emission in Asia. Journal of Environmental Mangement 72, 149-161.

Crutzen, P. J., Delany, A. C., Greenberg, J., Haagenson, P., Heidt, L., Leub, R. Pollock, W., Seiler, W., Wartburg, A. and Zimmerman, P. (1985). Tropospheric chemical composition measurements in Brazil during the dry season. *Journal Atmospheric Chemistry*, 2, 233-256.

Griggs, M. (1975). Measurements of the atmospheric aerosol optical thickness over water using ERTS-1 data. J. Air Pollution Control Assessment, Vol. 25, 622-626.

Hansen, J. E. and Lacis, A. A. (1990). Sun and Dust Versus Greenhouse Gaseous: An Assessment of Their Relative Roles in Global Climate Change. *Nature*, 346, 713-719.

Holben, B. N., Eric Vermote, Kaufman, Y. J., Tanre, D., and Kalb, V. (1992). Aerosol Retrieval over Land from AVHRR Data-Application for Atmospheric Correction. IEEE Transaction on Geoscience and Remote Sensing, Vol. 30, No. 2, 212-221.

Isakov, V. Y., Feind, R. E., Vasilyev, O. B. and Welch, R. M. (1996). Retrieval of Aerosol Spectral Optical Thickness from AVIRIS Data. IEEE.

Kaufman, Y. J., Tanre, D., Boucher, O. (2002). A Satellite View of Aerosols in the Climate System. Nature, Vol. 419, 215-223.

Lacis, A. A. and Mishchenko, M. I. (1995). Climate forcing, climate sensitivity, and climate response: A Radiative Modeling Perspective on Atmospheric Aerosols. *Aerosol Forcing Climate*. Pp 11-42, John Wiley, New York.

Ortiz, V., Figueroa, M., Picon, A. (2003). Aerosol and Cloud Properties Retrieval Using MODIS and MISR. NOAA-CREST/NASA-EPSCoR Joint Symposium for Climate Studies.

Paronis, D. and Sifakis N. (2003). Satellite Aerosol Optical Thickness Retrieval Over Land With Contrast Reduction Analysis Using A Variable Window Size. IEEE

Penner, J. E., Dickinson, R. E., and O'Neill, C. A., (1992). Effects of aerosol from biomass burning on the global radiation budget. *Science*, 256, 1432-1433.

Reid, J. P. and Sayer, R. M. (2002). Chemistry In The Clouds: The Role of Aerosols In Atmospheric Chemistry. *Science Progress(2002)*, 85(3), 263-296.

Sifakis, N., Soulakellis, N. Gkoufa, A. (1988). Manual of EO Image Processing Codes.

Sifakis, N., Soulakellis, N., Paronis, D. and Mavrantza, R. (2002). Manual of EO Image Processing Codes, Revised Reference Manual V.1.1.

Tanre, D., Deschamps, P. Y., Devaus, C. and Herman, M. (1993). Estimation of the Saharan Aerosol Optical Depth From Blurring Effects in Thematic Mapper Data. Journal of Geophysical Research, 15955-15964.

Tanre, D., Holben, B. N., Kaufman, Y. J. (1992). Atmospheric Correction Algorithm for NOAA-AVHRR Products: Theory and Application. IEEE Transaction on Geoscience and Remote Sensing, Vol. 30, No. 2, 231-248.